Synthesis and Electrochemical–EPR Investigation of the 48/49-Electron $[(\eta^5\text{-}C_5H_4Me)MnFe_2(\eta^5\text{-}C_5H_5)_2(\mu\text{-}CO)_2(\mu\text{-}NO)(\mu_3\text{-}NO)]^n$ Series (n = 0, 1–): Stereochemical-Bonding Analysis of the Redox-Generated Change in Geometry of a Triangular Mixed-Metal Cluster

Kimberly A. Kubat-Martin,[1a] Brock Spencer,[1b] and Lawrence F. Dahl*

Department of Chemistry, University of Wisconsin—Madison, Madison, Wisconsin 53706

Received June 11, 1986

A designed high-yield synthesis of a metal cluster containing a triply bridging nitrosyl ligand has been achieved via the cycloaddition of a 16-electron $Mn(\eta^5\text{-}C_5H_4Me)(CO)_2$ fragment to the 32-electron $Fe_2(\eta^5\text{-}C_5H_5)_2(\mu\text{-}NO)_2$, which formally possesses an Fe–Fe double bond, to give (in 76% yield) the 48-electron ON-capped $(\eta^5\text{-}C_5H_4Me)MnFe_2(\eta^5\text{-}C_5H_5)_2(\mu\text{-}CO)_2(\mu\text{-}NO)(\mu_3\text{-}NO)$ (**1**). Electrochemical measurements indicate that **1** can undergo a reversible one-electron oxidation to the 47-electron monocation ($\mathbf{1}^+$) and a reversible one-electron reduction to the 49-electron monoanion ($\mathbf{1}^-$). An attempted oxidation of **1** to $\mathbf{1}^+$ with $AgPF_6$ instead gave rise (in 10% yield) to the 48-electron HN-capped $[(\eta^5\text{-}C_5H_4Me)MnFe_2(\eta^5\text{-}C_5H_5)_2(\mu\text{-}CO)_2(\mu\text{-}NO)(\mu_3\text{-}NH)]^+$ monocation (**2**) via a ligand transformation of the π-acceptor μ_3-NO ligand into an electronically equivalent π-donor μ_3-NH^+ ligand. The 49-electron monoanion ($\mathbf{1}^-$) of **1** was obtained (in 44% yield) by the reduction of **1** with potassium–benzophenone and was isolated as the $[K(2,2,2\text{-crypt})]^+$ salt. X-ray crystallographic studies of the 48-electron neutral parent (**1**) and its monoanion ($\mathbf{1}^-$) revealed that the central $MnFe_2(\mu\text{-}CO)_2(\mu\text{-}NO)(\mu_3\text{-}NO)$ core in both **1** and $\mathbf{1}^-$ closely conforms to C_s—m symmetry with the mirror plane passing through the Mn atom and the doubly and triply bridging nitrosyl ligands which symmetrically link the two mirror-related Fe atoms. The redox-generated changes in geometry together with EPR data of $\mathbf{1}^-$ provide conclusive evidence that the unpaired electron in $\mathbf{1}^-$ occupies a nondegenerate HOMO which is primarily antibonding between the two iron atoms. This conclusion is based upon the Fe–Fe edge of the isosceles $MnFe_2$ triangle greatly enlarging by 0.164 Å from 2.441 (2) in **1** to 2.605 (3) Å in $\mathbf{1}^-$ in contrast to the two chemically equivalent Mn–Fe edges slightly decreasing by 0.013 Å from 2.561 (av) in **1** to 2.548 Å (av) in $\mathbf{1}^-$. This particular distortion of the $MnFe_2$ framework is consistent with EPR solution spectra of $\mathbf{1}^-$ each exhibiting a single narrow line (29-G and 25-G widths at 22 and −40 °C, respectively) at g = 1.968 (5) with no evidence of hyperfine coupling due to the interaction of the unpaired electron with either the ^{55}Mn nucleus (100% abundance, $I = {}^5/_2$) or a ^{14}N nucleus (99.63% abundance, I = 1). $(\eta^5\text{-}C_5H_4Me)MnFe_2(\eta^5\text{-}C_5H_5)_2(\mu\text{-}CO)_2(\mu\text{-}NO)(\mu_3\text{-}NO)$: M_r 491.98; monoclinic; $P2_1/c$; a = 16.67 (1) Å, b = 7.974 (4) Å, c = 14.887 (7) Å, β = 115.92 (4) Å, V = 1780 (1) Å^3 at T = 295 K; d_{calcd} = 1.81 g/cm^3 for Z = 4; anisotropic least-squares refinement (SHELXTL) converged at $R_1(F)$ = 3.6% and $R_2(F)$ = 5.2% for 3639 independent reflections ($I > 3\sigma(I)$). $[K(2,2,2\text{-crypt})]^+[(\eta\text{-}C_5H_4Me)MnFe_2(\eta^5\text{-}C_5H_5)_2(\mu\text{-}CO)_2(\mu\text{-}NO)(\mu_3\text{-}NO)]^-$: M_r 907.58; triclinic; $P\bar{1}$; a = 10.351 (7) Å, b = 13.010 (9) Å, c = 15.750 (9) Å, α = 102.51 (5)°, β = 103.14 (5)°, γ = 94.90 (6)°, V = 1996 (2) Å^3 at T = 203 K; d_{calcd} = 1.50 g/cm^3 for Z = 2; anisotropic least-squares refinement (SHELXTL) converged at $R_1(F)$ = 6.9% and $R_2(F)$ = 7.1% for 2868 independent reflections ($I > 3\sigma(I)$).

Introduction

Our investigation[2] of the rational syntheses of mixed-metal cluster compounds via metal-fragment additions to the 32-electron $Co_2(\eta^5\text{-}C_5H_5)_2(\mu\text{-}CO)_2$[3] has been recently extended to a study[4] of the reactivity of the 32-electron $Fe_2(\eta^5\text{-}C_5H_5)_2(\mu\text{-}NO)_2$.[5] Since metal-fragment cycloadditions of $Co_2(\eta^5\text{-}C_5Me_5)_2(\mu\text{-}CO)_2$ gave rise to triangular mixed-metal clusters containing triply bridging carbonyl ligands,[2] it was assumed that corresponding cycloadditions of metal fragments to the isoelectronic $Fe_2(\eta^5\text{-}C_5H_5)_2(\mu\text{-}NO)_2$ should yield triangular metal clusters containing triply bridging nitrosyl ligands. This possible preparative route was of particular interest because metal clusters containing capping nitrosyl groups are relatively rare. The few known metal clusters with μ_3-NO ligands include $Mn_3(\eta^5\text{-}C_5H_{5-x}Me_x)_3(\mu\text{-}NO)_3(\mu_3\text{-}NO)$ (x = 0,[6] 1[7]) by the photochemical or thermal decarbonylation of $Mn_2(\eta^5\text{-}C_5H_{5-x}Me_x)_2(CO)_2(NO)_2$ (x = 0, 1), $M_3(\eta^5\text{-}C_5H_{5-x})_3(\mu_3\text{-}NO)_2$ (M = Rh, x = 0;[8] M = Co, x = 0,[9a] 1[9b]) by the thermolysis

(1) (a) Based in part on the Ph.D. thesis of K. A. Kubat-Martin at the University of Wisconsin—Madison, June, 1986. Present address: Los Alamos Scientific Laboratory, University of California, Los Alamos, NM 87545. (b) On sabbatical leave (June 1985–Dec 1985) at UW—Madison from Department of Chemistry, Beloit College, Beloit, WI 53511.

(2) Cirjak, L. M.; Huang, L.-S.; Zhu, Z.-H.; Dahl, L. F. *J. Am. Chem. Soc.* **1980**, *102*, 6623–6626.

(3) (a) Bailey, W. I., Jr.; Collins, D. M.; Cotton, F. A.; Baldwin, J. C.; Kaska, W. C. *J. Organomet. Chem.* **1979**, *165*, 373–381. (b) Ginsburg, R. E.; Cirjak, L. M.; Dahl, L. F. *J. Chem. Soc., Chem. Commun.* **1979**, 468–470. (c) Schore, N. E. *J. Organomet. Chem.* **1979**, *173*, 301–316. (d) Cirjak, L. M.; Ginsburg, R. E.; Dahl, L. F. *Inorg. Chem.* **1982**, *21*, 940–957 and references cited therein. (e) Dudeney, N.; Green, J. C.; Kirchner, O. N.; Smallwood, F. St. J. *J. Chem. Soc., Dalton Trans.* **1984**, 1883–1887.

(4) (a) Kubat-Martin, K. A.; Rae, A. D.; Dahl, L. F. *Abstracts of Papers*, 187th National Meeting of the American Chemical Society, St. Louis, MO: American Chemical Society, Washington, DC, 1984. (b) Kubat-Martin, K. A.; Dahl, L. F. *Abstracts of Papers*, 190th National Meeting of the American Chemical Society, Chicago, IL; American Chemical Society; Washington, DC, 1985.

(5) (a) Brunner, H. *J. Organomet. Chem.* **1968**, *14*, 173–178. (b) Calderon, J. L.; Fontana, S.; Frauendorfer, D.; Day, V. W.; Iske, S. D. A. *J. Organomet. Chem.* **1974**, *64*, C16–C18.

(6) (a) Elder, R. C. *Inorg. Chem.* **1974**, *13*, 1037–1042. (b) Elder, R. C.; Cotton, F. A.; Schunn, R. A. *J. Am. Chem. Soc.* **1967**, 3645–3646. (c) King, R. B.; Bisnette, M. B. *Inorg. Chem.* **1964**, *3*, 791–796.

(7) Kolthammer, B. W. S.; Legzdins, P. *J. Chem. Soc., Dalton, Trans*, **1978**, 31–35.

(8) Dimas, P. A.; Lawson, R. J.; Shapley, J. R. *Inorg. Chem.* **1981**, *20*, 281–283.

(9) (a) Müller, J.; Schmitt, S. *J. Organomet. Chem.* **1975**, *97*, C54–C56. (b) Kubat-Martin, K. A.; Rae, A. D.; Dahl, L. F. *Organometallics* **1985**, *4*, 2221–2223.

0276-7333/87/2306-2580$01.50/0

of the corresponding $M_2(\eta^5\text{-}C_5H_{5-x}Me_x)_2(\mu\text{-}NO)_2$, and the $[Co_3(\eta^5\text{-}C_5H_{5-x}Me_x)_3(\mu_3\text{-}NH)(\mu_3\text{-}NO)]^+$ monocations (x = 0, 1)[10] by the direct replacement of a μ_3-CO ligand in $Co_3(\eta^5\text{-}C_5H_{5-x}Me_x)_3(\mu_3\text{-}NH)(\mu_3\text{-}CO)$ (x = 0, 1) with an isoelectronic μ_3-NO^+ ligand by reaction with NO^+ ion.

Unfortunately, our initial work showed that the photochemical generation of several 16-electron metal fragments by loss of CO from their metal carbonyl precursors resulted in the $Fe_2(\eta^5\text{-}C_5H_5)_2(\mu\text{-}NO)_2$ reacting primarily with the liberated carbon monoxide instead of with the metal fragment to give $Fe_2(\eta^5\text{-}C_5H_5)_2(\mu\text{-}CO)_2(CO)_2$ (in high yields) rather than the desired nitrosyl-capped addition-type product. In order to circumvent this problem, an adduct species which can readily lose a solvent molecule was used to generate an intermediate metal fragment system. This methodology was applied in the designed synthesis[4b] of $(\eta^5\text{-}C_5H_4Me)MnFe_2(\eta^5\text{-}C_5H_5)_2(\mu\text{-}CO)_2(\mu\text{-}NO)(\mu_3\text{-}NO)$ (1) by the addition of the 16-electron $Mn(\eta^5\text{-}C_5H_4Me)(CO)_2$ fragment (formed from $Mn(\eta^5\text{-}C_5H_4Me)(CO)_2$·THF) across the formal Fe–Fe double bond of $Fe_2(\eta^5\text{-}C_5H_5)_2(\mu\text{-}NO)_2$. The resulting air-stable 1, formed in 76% yield, represents the first triangular mixed-metal cluster which contains a triply bridging nitrosyl ligand.

On the basis of our electrochemical investigations of other OC- and ON-capped triangular metal clusters (most notably the $[Co_3(\eta^5\text{-}C_5H_{5-x}Me_x)_3(\mu_3\text{-}NO)_2]^n$ series (x = 0, 1; n = 1+, 0, 1−),[9b] the $[Ni_3(\eta^5\text{-}C_5H_{5-x}Me_x)_3(\mu_3\text{-}CO)_2]^n$ series (x = 0, 1, 5; n = 1+, 0, 1−),[11] the corresponding $[(\eta^5\text{-}C_5Me_5)CoNi_2(\eta^5\text{-}C_5H_5)_2(\mu_3\text{-}CO)_2]^n$ series (n = 0, 1-)[11a,b] and the $[Co_3(\eta^5\text{-}C_5H_4Me)_3(\mu_3\text{-}NH)(\mu_3\text{-}NO)]^n$ series (n = 1+, 0)[10]), we assumed that 1 would also display reversible redox behavior.

Cyclic voltammetric measurements of 1 indicated reversible electrochemical processes that consist of a one-electron oxidation to its 47-electron monocation (1^+) and a one-electron reduction to its 49-electron monoanion. The monanion (1^-) was isolated from a potassium–benzophenone reduction as the $[K(2,2,2\text{-crypt})]^+$ salt. Attempts to oxidize 1 to 1^+ have led instead to the isolation of a ligand-transformation product (2) in which the three-electron donating μ_3-NO ligand in 1 was replaced by a three-electron donating $(\mu_3\text{-}NH)^+$ ligand in 2.

Herein are presented the details of the synthesis and characterization (including crystallographic determinations) of 1 and 1^-. The electronic implications of an analysis of the geometrical differences between 1 and 1^- and the EPR data for 1^- are also given.

Experimental Section

Materials and Measurements. All reactions, solution transfers, and sample manipulations were performed on a preparative vacuum line under nitrogen or argon or within a Vacuum Atmospheres glovebox with oven- or flame-dried standard Schlenk-type glassware. The following solvents were dried, freshly distilled, and degassed prior to use: octane (CaH_2), THF (potassium–benzophenone), toluene (sodium–benzophenone), CH_2Cl_2 (CaH_2), and hexane (CaH_2). $Fe_2(\eta^5\text{-}C_5H_5)_2(\mu\text{-}NO)_2$ was synthesized via a variation of the method of Brunner;[5] the potassium/benzophenone reducing agent was synthesized by a stirring of a THF solution of equimolar amounts of potassium and benzophenone in a flame-dried round-bottom flask for 8 h. The 2,2,2-cryptand (which denotes $N(C_2H_4OC_2H_4OC_2H_4)_3N$) was purchased from the Parish Chemical Co. All other reagents were purchased from major chemical suppliers and used without further purification.

NMR spectra were recorded on a Bruker WP-200 spectrometer; Infrared spectra were obtained with a Beckman 4240 spectrophotometer. Cyclic voltammograms were obtained with a BAS-100 electrochemical analyzer with the electrochemical cell enclosed in an N_2-filled Vacuum Atmospheres glovebox. EPR data were obtained with a Varian E-15 spectrometer; DPPH was used as a standard for g-value determinations. Glass samples were made by a quenching of dilute solutions in liquid N_2; low-temperature spectra were checked for possible power saturation. Mass spectral data were recorded on a Nicolet MS-1000 mass spectrometer via an electron-impact mode (15 eV).

Preparation and Physical Properties of $(\eta^5\text{-}C_5H_4Me)MnFe_2(\eta^5\text{-}C_5H_5)_2(\mu\text{-}CO)_2(\mu\text{-}NO)(\mu_3\text{-}NO)$ (1). Since photolytic generation of a 16-electron metal fragment by loss of carbon monoxide from a chemical precursor in the presence of $Fe_2(\eta^5\text{-}C_5H_5)_2(\mu\text{-}NO)_2$ resulted in the undesired formation of $Fe_2(\eta^5\text{-}C_5H_5)_2(\mu\text{-}CO)_2(CO)_2$, $Mn(\eta^5\text{-}C_5H_4Me)(CO)_2$·THF was synthesized separately and then added to the iron nitrosyl dimer. $Mn(\eta^5\text{-}C_5H_4Me)(CO)_3$ (0.5 mL, 350 mg, 1.6 mmol) was dissolved in ca. 300 mL of THF and was transferred to a water-cooled Pyrex photolysis apparatus. Additional cooling and protection against extensive solvent loss were provided by a dry ice/acetone-cooled condenser. The solution was irradiated for approximately 5 h with a Hanovia 450-W medium-pressure Hg vapor lamp. A slow stream of N_2, which was bubbled through the reaction mixture, stirred the solution in addition to facilitating the removal of evolved CO.

The resulting solution containing $Mn(\eta^5\text{-}C_5H_4Me)(CO)_2$·THF and some unreacted $Mn(\eta^5\text{-}C_5H_4Me)(CO)_3$ was concentrated under vacuum to a volume of 200 mL and then added to a flask containing $Fe_2(\eta^5\text{-}C_5H_5)_2(\mu\text{-}NO)_2$ (484 mg, 1.6 mmol). This solution was stirred at room temperature for 12 h, after which the THF was stripped under vacuum from the products. The contents of the flask were then dissolved in toluene and chromatographed on an alumina column (80–200 mesh neutral alumina, Brockman activity I) which had been packed in toluene.

Three bands were eluted from the column. The first, a yellow band, and the second, a green band, were identified from IR spectra as unreacted starting materials—viz., $Mn(\eta^5\text{-}C_5H_4Me)(CO)_3$ and $Fe_2(\eta^5\text{-}C_5H_5)_2(\mu\text{-}NO)_2$, respectively. A greenish brown third band was then removed from the column with a 50/50 toluene/THF solvent mixture. Both solvents were removed by evaporation under a N_2 stream, and the crystalline product was washed with hexane. A 76% yield of the desired $(\eta^5\text{-}C_5H_4Me)MnFe_2(\eta^5\text{-}C_5H_5)_2(\mu\text{-}CO)_2(\mu\text{-}NO)(\mu_3\text{-}NO)$ (590 mg, 1.2 mmol) was obtained. Crystals of 1 suitable for X-ray diffraction study were grown by dissolving 1 in THF followed by carefully layering hexane over the THF solution.

A solid-state spectrum of 1 (taken as a KBr pellet) exhibited bridging carbonyl bands at 1828 and 1792 cm^{-1}, a doubly bridging nitrosyl band at 1515 cm^{-1}, and a triply bridging nitrosyl band at 1315 cm^{-1} (Figure 1, supplementary material). A solution spectrum in THF showed carbonyl bands at 1843 and 1800 cm^{-1} and nitrosyl bands at 1525 and 1335 cm^{-1}.

A ^1H NMR spectrum of 1 in $CDCl_3$ displayed two equivalent sets of cyclopentadienyl ring proton resonances centered at δ 4.71 (2 H) and 4.76 (2 H), a cyclopentadienyl ring proton resonance at δ 4.59 (10 H), and a single methyl proton resonance at δ 1.96 (3 H).

A mass spectrum of 1 (electron impact, 15 eV) showed the existence of the parent ion peak (m/e 492) with other prominent peaks assigned to the $[(C_5H_4Me)MnFe_2(C_5H_5)_2(NO)_2]^+$ fragment (m/e 436), the $[(C_5H_4Me)MnFe_2(C_5H_5)_2(NO)]^+$ fragment (m/e 406), the $[(C_5H_4Me)MnFe_2(C_5H_5)(NO)_2]^+$ fragment (m/e 315), and the $[Fe_2(C_5H_5)_2(NO)]^+$ fragment (m/e 272).

Electrochemistry of $(\eta^5\text{-}C_5H_4Me)MnFe_2(\eta^5\text{-}C_5H_5)_2(\mu\text{-}CO)_2(\mu\text{-}NO)(\mu_3\text{-}NO)$ (1). Cyclic voltammetric measurements were carried out either in THF/0.1 M $[NBu_4]^+[PF_6]^-$ or in CH_2Cl_2/0.1 M $[NBu_4]^+[PF_6]^-$. The working electrode was a platinum disk; the reference electrode was a Vycor-tipped aqueous

(10) (a) Bedard, R. L.; Rae, A. D.; Dahl, L. F. *J. Am. Chem. Soc.* **1986**, *108*, 5924–5932. (b) Bedard, R. L.; Dahl, L. F. *J. Am. Chem. Soc.* **1986**, *108*, 5942–5948.

(11) (a) $Ni_3(\eta^5\text{-}C_5H_5)_3(\mu_3\text{-}CO)_2$ (X-ray data) and $(\eta^5\text{-}C_5H_{5-x}Me_x)CoNi_2(\eta^2\text{-}C_5H_5)_2(\mu_3\text{-}CO)_2$ (where x = 0, 1, 5) (synthesis, X-ray data, CV); Byers, L. R.; Uchtmann, V. A.; Dahl, L. F. *J. Am. Chem. Soc.* **1981**, *103*, 1942–1951. (b) $[Ni_3(\eta^5\text{-}C_5H_5)_3(\mu_3\text{-}CO)_2]^-$, $[Ni_3(\eta^5\text{-}C_5Me_5)_3(\mu_3\text{-}CO)_2]^n$ (where n = 2+, 1+, 0, 1−), and $[(\eta^5\text{-}C_5Me_5)CoNi_2(\eta^5\text{-}C_5H_5)_2(\mu_3\text{-}CO)_2]^-$: Maj, J. A.; Rae, A. D.; Dahl, L. F. *J. Am. Chem. Soc.* **1982**, *104*, 3054–3063. (c) $Ni_3(\eta^5\text{-}C_5H_4Me)_3(\mu_3\text{-}CO)_2$ (synthesis, X-ray data): Englert, M. L.; Dahl, L. F., to be submitted for publication. (d) $[Ni_3(\eta^5\text{-}C_5H_{5-x}Me_x)_3(\mu_3\text{-}CO)_2]^n$ (where x = 0, 1; n = 1+, 0, 1−) (CV): Bedard, R. L.; Dahl, L. F. *J. Am. Chem. Soc.* **1986**, *108*, 5933–5942.

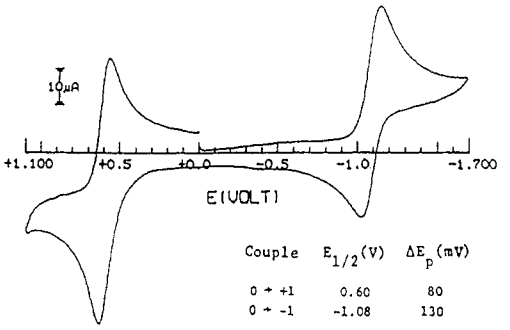

Figure 2. Cyclic voltammogram of $(\eta^5\text{-}C_5H_4Me)MnFe_2(\eta^5\text{-}C_5H_5)_2(\mu\text{-}CO)_2(\mu\text{-}NO)(\mu_3\text{-}NO)$ (1) showing that this neutral parent can undergo a one-electron reduction to its monoanion 1^- and a one-electron oxidation to its monocation (1^+). This CV was carried out in CH_2Cl_2/0.1 M $[NBu_4]^+[PF_6]^-$ at a platinum disk electrode.

SCE separated from the test solution by a Vycor-tipped salt bridge filled with a 0.1 M $TBAPF_6$ solution. The counter electrode was a platinum coil. The solution volumes were about 5 mL of either THF or CH_2Cl_2 containing approximately 10^{-3} M 1. Figure 2 shows a typical cyclic voltammogram of 1 in CH_2Cl_2 with a scan rate of 200 mV/s.

Formation of the HN-Capped $[(\eta^5\text{-}C_5H_4Me)MnFe_2(\eta^5\text{-}C_5H_5)_2(\mu\text{-}CO)_2(\mu\text{-}NO)(\mu_3\text{-}NH)]^+$ Monocation (2) from an Attempted Oxidation of $(\eta^5\text{-}C_5H_4Me)MnFe_2(\eta^5\text{-}C_5H_5)_2(\mu\text{-}CO)_2(\mu\text{-}NO)(\mu_3\text{-}NO)$ (1). Neutral 1 (100 mg, 0.20 mmol) was dissolved in 50 mL of CH_2Cl_2 and transferred via cannulae into a slurry of $AgPF_6$ (51 mg, 0.20 mmol) in CH_2Cl_2. This solution was stirred, and the reaction was monitored by IR spectroscopy. After 20 min, an IR spectrum still showed carbonyl and nitrosyl bands associated with the neutral triangle (along with bands from a new species); another equivalent of $AgPF_6$ was then added to the solution. After an additional 20 min of stirring, IR data indicated a total conversion of the starting material into a new species which exhibited doubly bridging carbonyl and nitrosyl bands at expectedly higher wavenumbers. However, no band characteristic of a triply bridging nitrosyl ligand was observed. A CH_2Cl_2 solution containing the cationic product was filtered from the insoluble silver precipitates, and the solvent was removed under a stream of N_2. The product (10% yield) was washed with dry, degassed toluene and then redissolved in CH_2Cl_2. A solution infrared spectrum of **2** (CH_2Cl_2) exhibited two bridging carbonyl bands at 1895 and 1845 cm^{-1} and a bridging nitrosyl band at 1565 cm^{-1}. Crystals of the $[PF_6]^-$ salt of **2** were formed by layering hexane over the concentrated CH_2Cl_2 solution. The crystal structure and stoichiometry of this compound were established from an X-ray diffraction investigation; details will be presented elsewhere upon completion of further chemical studies.[12]

Preparation and Physical Properties of the $[K(2,2,2\text{-crypt})]^+$ Salt of the Reduced $[(\eta^5\text{-}C_5H_4Me)MnFe_2(\eta^5\text{-}C_5H_5)_2(\mu\text{-}CO)_2(\mu\text{-}NO)(\mu_3\text{-}NO)]^-$ Monoanion (1^-). A mixture of 1 (100 mg, 0.20 mmol) and 2,2,2-cryptand (77 mg, 0.20 mmol) was dissolved in ca. 50 mL of THF. This mixture was titrated with a solution of the reductant potassium–benzophenone in THF (215 mg, 5.5 mmol of K metal; 1000 mg, 5.5 mmol of benzophenone in 75 mL of THF); the reaction was monitored by IR spectra. Titration was continued until the carbonyl and nitrosyl bands associated with 1 had disappeared from the IR spectra and were replaced with new bands associated with 1^-. At this point, the THF was removed from the reaction mixture by evaporation under a stream of N_2, and the product was washed with rigorously degassed toluene (six freeze–pump–thaw degas cycles) to remove the benzophenone and any neutral starting material. A 44% yield of the monoanion was obtained. Crystals were formed by dissolving the monoanion in THF followed by carefully layering hexane over the THF solution.

A solution infrared spectrum of 1^- displayed two bridging carbonyl bands at 1760 and 1715 cm^{-1}, a doubly bridging nitrosyl band at 1355 cm^{-1}, and a triply bridging nitrosyl band (broad) at 1280 cm^{-1}. Figure 3 (supplementary material) shows the IR

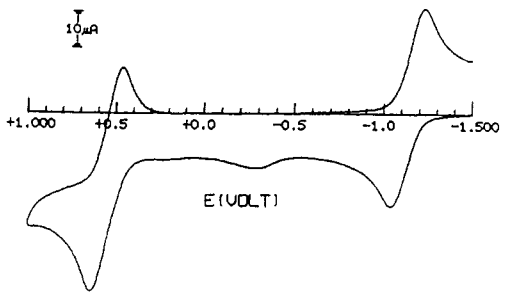

Figure 4. Cyclic voltammogram of the 49-electron $[(\eta^5\text{-}C_5H_4Me)MnFe_2(\eta^5\text{-}C_5H_5)_2(\mu\text{-}CO)_2(\mu\text{-}NO)(\mu_3\text{-}NO)]^-$ monoanion (1) as the $[K(2,2,2\text{-crypt})]^+$ salt. Two reversible one-electron oxidation couples are shown—viz., the first one to the 48-electron parent (1) and the second one to the 47-electron monocation (1^+). This CV was carried out in THF/0.1 M $[NBu_4]^+[PF_6]^-$ at a platinum disk electrode.

changes in the carbonyl region upon reduction of 1 to 1^-. A cyclic voltammogram of 1^- in THF (Figure 4) showed the existence of two redox processes. The first couple, at $E_{1/2} = -1.14$ V, involves a one-electron oxidation of the monoanion to the neutral 1. The second couple, at $E_{1/2} = 0.55$ V, involves the oxidation of the neutral 1 to its 47-electron monocation.

EPR Spectra of $[K(2,2,2\text{-crypt})]^+[(\eta^5\text{-}C_5H_4Me)MnFe_2(\eta^5\text{-}C_5H_5)_2(\mu\text{-}CO)_2(\mu\text{-}NO)(\mu_3\text{-}NO)]^-$. EPR spectra of 1^- in THF consisted of a single line (without hyperfine structure) at $g = 1.968$ (5) with a 29-G line width at room temperature which narrowed to 25 G at approximately −40 °C. A frozen-glass EPR spectrum at −110 °C exhibited two principal g values (viz., $g_\parallel = 1.89$; $g_\perp = 2.00$) with a line-shape characteristic of an axially symmetric spin $^1/_2$ system; the value of 1.96 for the average isotropic $g = g_\parallel + 2g_\perp$ is in reasonable agreement with the solution g value of 1.97.

Structural Determination of $(\eta^5\text{-}C_5H_4Me)MnFe_2(\eta^5\text{-}C_5H_5)_2(\mu\text{-}CO)_2(\mu\text{-}NO)(\mu_3\text{-}NO)$ (1). A large dark brown crystal of approximate dimensions 1.5 × 2.0 × 2.0 mm was cleaved to obtain a parallelepiped-shaped crystal measuring 0.8 × 0.7 × 0.6 mm. This crystal was attached via epoxy resin to a glass fiber and mounted inside an argon-filled Lindemann glass capillary which was then flame-sealed. A P3F Nicolet diffractometer with Mo Kα radiation was utilized in the X-ray diffraction measurements. The crystal system was determined from diffraction data to be monoclinic; the dimensions and the symmetry of the chosen cell were verified from axial photographs. The setting angles for 25 well-centered high-angle reflections yielded refined lattice constants at 22 °C of $a = 16.67$ (1) Å, $b = 7.974$ (4) Å, $c = 14.887$ (7) Å, and $\beta = 115.92$ (4)°. The cell volume is 1780 (1) Å^3; the calculated density for $Z = 4$ and a formula weight of 491.98 is 1.81 g/cm^3. Further information concerning the procedures involved in crystal aligment and data collection is given elsewhere.[13] Intensity data for two reciprocal lattice octants ($\pm h,k,l$) were collected via the ω-scan mode at variable scan speeds (4.0–29.0°/min) over a 2θ scan range of 3.0–55.0°.

The intensities of three standard reflections did not vary significantly during data collection. A merging of 4083 measured intensities gave rise to 3639 independent observed reflections ($I > 3.0\sigma(I)$ which were used in the structural determination and refinement. An empirical absorption correction[14] ($\mu = 23.11$ cm^{-1} for Mo Kα radiation) was made. Systematic absences of $h0l$ for l odd and $0k0$ for k odd uniquely indicated the probable space group to be $P2_1/c$ (C_{2h}^5—No. 14) which results in one crystallographically independent molecule. The crystal structure was determined by direct methods (SHELXTL[15]) and refined by least squares. A crystal disorder of the methylcyclopentadienyl group (involving two superimposed ring orientations with different positions for the methyl substituent) was modeled by refinement

(12) Barr, M. E.; Kubat-Martin, K. A.; Dahl, L. F., in preparation.

(13) Byers, L. R.; Dahl, L. F. *Inorg. Chem.* **1980**, *19*, 277–284.

(14) Höpe, H., personal communication (Feb 1984) to L. F. Dahl. The Höpe program ABSORPTION (Höpe, H.; Moezzi, B., unpublished results) utilizes an empirical absorption tensor from an expression relating $|F_o|$ and $|F_c|$.

(15) Programs used were those of SHELXTL (1984 version). Computations were performed on an Eclipse S/4 system.

Table I. Atomic Coordinates (× 10^4) and Equivalent Isotropic Thermal Parameters[a] (Å² × 10^3) for the Non-Hydrogen Atoms of $(\eta^5\text{-}C_5H_4Me)MnFe_2(\eta^5\text{-}C_5H_5)_2(\mu\text{-}CO)_2(\mu\text{-}NO)(\mu_3\text{-}NO)$ (1)

	x	y	z	U
Mn	2556 (1)	11039 (1)	3122 (1)	28 (1)
Fe(1)	3061 (1)	9198 (1)	2060 (1)	24 (1)
Fe(2)	1574 (1)	8737 (1)	1949 (1)	27 (1)
N(123)	2701 (1)	8699 (3)	3081 (2)	27 (1)
O(123)	3007 (1)	7593 (3)	3745 (1)	38 (1)
N(12)	1950 (1)	9353 (3)	1030 (2)	29 (1)
O(12)	1637 (1)	9507 (3)	129 (2)	46 (1)
C(1)	2962 (2)	11834 (4)	2237 (2)	36 (1)
O(1)	3171 (2)	12907 (3)	1853 (2)	59 (1)
C(2)	1420 (2)	11371 (4)	2099 (2)	38 (1)
O(2)	798 (2)	12186 (3)	1618 (2)	57 (1)
C(11)	4028 (2)	9670 (5)	1544 (3)	55 (2)
C(12)	4447 (2)	9488 (6)	2588 (3)	61 (2)
C(13)	4284 (2)	7905 (6)	2820 (3)	60 (2)
C(14)	3731 (2)	7043 (4)	1927 (3)	54 (2)
C(15)	3591 (2)	8171 (5)	1139 (3)	49 (1)
C(21)	193 (2)	8382 (6)	1160 (3)	65 (2)
C(22)	637 (2)	7060 (5)	949 (3)	57 (1)
C(23)	1146 (2)	6227 (4)	1857 (3)	54 (2)
C(24)	1010 (2)	7015 (5)	2615 (3)	53 (1)
C(25)	424 (2)	8357 (5)	2177 (4)	63 (2)
C(31)	2846 (3)	13384 (5)	3891 (3)	67 (2)
C(32)	2165 (3)	12653 (6)	4002 (3)	75 (2)
C(33)	2458 (3)	11109 (6)	4509 (3)	70 (2)
C(34)	3364 (3)	10948 (4)	7407 (2)	51 (1)
C(35)	3603 (2)	12368 (5)	4322 (2)	51 (1)
Me	1818 (5)	10221 (11)	4749 (5)	71 (3)
Me′	4400 (6)	13107 (16)	4327 (6)	72 (4)

[a] The equivalent isotropic U is defined as one-third the trace of the orthogonalized U_{ij} tensor.

of the site occupancy factor for the two methyl carbon positions (i.e., a random distribution between both sites corresponding to $\alpha = 0.5$ was found). The C_5H_5 and C_5H_4Me rings were not constrained; hydrogen atoms were inserted at idealized positions and included in the refinement as fixed-atom contributors. The last least-squares cycle converged to $R_1(F) = 3.6\%$ and $R_2(F) = 5.2\%$. A final difference Fourier map did not reveal any unusual features; the final data-to-parameter ratio was 14.4/1.

Atomic coordinates and isotropic temperature parameters for the non-hydrogen atoms are listed in Table I. Selected interatomic distances and bond angles are shown in Table II. Tables of coordinates and isotropic temperature factors for the hydrogen atoms and anisotropic thermal parameters for the non-hydrogen atoms and a listing of observed and calculated structure factor amplitudes are available as supplementary material.

Structural Determination of $[K(2,2,2\text{-crypt})]^+[(\eta^5\text{-}C_5H_4Me)MnFe_2(\eta^5\text{-}C_5H_5)_2(\mu\text{-}CO)_2(\mu\text{-}NO)(\mu_3\text{-}NO)]^-$. Crystals of the $[K(2,2,2\text{-crypt})]^+$ salt of 1^- were examined under a 50/50 mixture of Paratone-N and mineral oil. A small plate-like crystal of dimensions 0.5 × 0.2 × 0.1 mm was connected via epoxy resin to a glass fiber mounted inside an argon-filled Lindemann capillary which was then flame-sealed. Diffraction data revealed the crystal to be triclinic; refined lattice constants at −70 °C of $a = 10.351$ (7) Å, $b = 13.010$ (9) Å, $c = 15.750$ (9) Å = 102.51 (5)°, $\beta = 103.14$ (5)°, and $\gamma = 94.90$ (6)° were determined from the setting angles of 25 centered reflections. Axial photographs verified the dimensions of the chosen triclinic cell. The cell volume is 1996 (2) Å³; the calculated density for $Z = 2$ and a formula weight of 907.58 is 1.50 g/cm³. Intensity data ($h,\pm k,\pm l$) were collected with Mo Kα radiation on a P3F diffractometer via the θ–2θ scan mode at variable scan speeds (2.0–29.0°/min) over a 2θ range of 4.0–45.0°. Since linear decreases of ca. 5% in the intensities of the three standard reflections were detected during data collection, a decay correction was applied to the 5594 collected data. A merging of these data yielded 2868 independent reflections ($I > 3.0\sigma(I)$) which were used in the structural determination and refinement. An empirical absorption correction[14] ($\mu = 11.78$ cm^{-1} for Mo Kα radiation) was made. The crystal structure was determined under $P\bar{1}$ symmetry by direct methods (SHELXTL[15]) and refined by least squares. Each of the rings for the C_5H_5 and C_5H_4Me ligands was constrained to fivefold symmetry with C–C and C–H distances of 1.420 and 0.96 Å, respectively. The hydrogen atoms in the $[K(2,2,2\text{-crypt})]^+$ counterion were also inserted at idealized positions and refined as fixed-atom contributors. All non-hydrogen atoms were refined with individual anisotropic thermal parameters. Refinement converged at $R_1(F) = 6.9\%$ and $R_2(F) = 7.1\%$. A final difference map did not reveal any anomalous features; the final data-to-parameter ratio was 6.2/1.

Table II. Selected Distances and Bond Angles for $(\eta^5\text{-}C_5H_4Me)MnFe_2(\eta^5\text{-}C_5H_5)_2(\mu\text{-}CO)_2(\mu\text{-}NO)(\mu_3\text{-}NO)$ (1)

	Distances (Å)		
Fe(1)–Fe(2)	2.441 (2)	C(31)–C(32)	1.350 (7)
Fe(1)–Mn	2.555 (2)	C(32)–C(33)	1.414 (7)
Fe(2)–Mn	2.567 (2)	C(33)–C(34)	1.411 (7)
Fe(1)–N(123)	1.902 (3)	C(34)–C(35)	1.402 (6)
Fe(2)–N(123)	1.897 (2)	C(35)–C(31)	1.397 (5)
Mn–N(123)	1.885 (2)		1.395 (av)
Fe(1)–N(12)	1.819 (2)		
Fe(2)–N(12)	1.803 (3)	C(33)–Me	1.451 (11)
Fe(1)–C(1)	2.133 (3)	C(35)–Me′	1.451 (12)
Mn–C(1)	1.835 (4)		
Fe(2)–C(2)	2.139 (3)	Fe(1)–C(11)	2.100 (5)
Mn–C(2)	1.857 (3)	Fe(1)–C(12)	2.104 (4)
		Fe(1)–C(13)	2.117 (4)
N(123)–O(123)	1.254 (3)	Fe(1)–C(14)	2.106 (4)
N(12)–O(12)	1.212 (3)	Fe(1)–C(15)	2.094 (4)
C1–O(1)	1.164 (4)		2.106 (av)
C2–O(2)	1.167 (4)		
		Fe(2)–C(21)	2.097 (3)
C(11)–C(12)	1.402 (6)	Fe(2)–C(22)	2.099 (4)
C(12)–C(13)	1.367 (7)	Fe(2)–C(23)	2.109 (4)
C(13)–C(14)	1.419 (5)	Fe(2)–C(24)	2.137 (5)
C(14)–C(15)	1.412 (6)	Fe(2)–C(25)	2.111 (5)
C(15)–C(11)	1.392 (5)		2.111 (av)
	1.398 (av)		
		Mn–C(31)	2.134 (4)
C(21)–C(22)	1.400 (6)	Mn–C(32)	2.131 (6)
C(22)–C(23)	1.408 (5)	Mn–C(33)	2.139 (5)
C(23)–C(24)	1.393 (7)	Mn–C(34)	2.139 (3)
C(24)–C(25)	1.402 (5)	Mn–C(35)	2.152 (3)
C(25)–C(21)	1.387 (7)		2.139 (av)
	1.398 (av)		
	Bond Angles (deg)		
Fe(1)–Fe(2)–Mn	61.2 (1)	Fe(1)–N(12)–O(12)	136.4 (2)
Fe(2)–Fe(1)–Mn	61.8 (1)	Fe(2)–N(12)–O(12)	137.7 (2)
Fe(1)–Mn–Fe(2)	56.9 (1)	Fe(1)–N(12)–Fe(2)	84.7 (1)
Fe(1)–N(123)–O(123)	127.8 (2)	Fe(1)–C(1)–O(1)	127.4 (3)
Fe(2)–N(123)–O(123)	127.9 (2)	Mn–C(1)–O(1)	152.8 (3)
Mn–N(123)–O(123)	133.2 (2)	Fe(1)–C(1)–Mn	79.7 (1)
Fe(1)–N(123)–Fe(2)	80.0 (1)	Fe(2)–C(2)–O(2)	126.7 (2)
Fe(1)–N(123)–Mn	84.8 (1)	Mn–C(2)–O(2)	153.7 (3)
Fe(2)–N(123)–Mn	85.5 (1)	Fe(2)–C(2)–Mn	79.6 (1)

Table III contains atomic coordinates and isotropic temperature parameters for the non-hydrogen atoms, while Table IV contains selected interatomic distances and bond angles. Tables of coordinates and isotropic temperature factors for the hydrogen atoms and anisotropic thermal parameters for the non-hydrogen atoms and a listing of observed and calculated structure factor amplitudes are available as supplementary material.

Results and Discussion

Cyclic Voltammetric Measurements of $(\eta^5\text{-}C_5H_4Me)MnFe_2(\eta^5\text{-}C_5H_5)_2(\mu\text{-}CO)_2(\mu\text{-}NO)(\mu_3\text{-}NO)$ (1). A cyclic voltammogram of 1 in CH_2Cl_2 (Figure 2) exhibits a reversible one-electron oxidation with an $E_{1/2}$ value of 0.60 V and a reversible one-electron reduction with an $E_{1/2}$ value of −1.08 V. For a 200 mV/s scan rate, the peak separations are 80 and 130 mV, respectively. The chemical reversibility of the oxidation and reduction waves in each couple is evidenced by the ratio between the anodic and cathodic currents being essentially unity.

The fact the 1 undergoes both a reduction to its 49-electron monoanion (1^-) and an oxidation to its 47-electron monocation (1^+) is not surprising in light of similar elec-

Table III. Atomic Coordinates (×10⁴) and Equivalent Isotropic Thermal Parameters[a] (Å² × 10³) for the Non-Hydrogen Atoms of [K(2,2,2-crypt)]⁺[(η^5-C_5H_4Me)$MnFe_2$(η^5-C_5H_5)$_2$(μ-CO)$_2$(μ-NO)(μ_3-NO)]⁻

	x	y	z	U
		A. Monoanion (1⁻)		
Mn	4975 (2)	5660 (1)	2247 (1)	43 (1)
Fe(1)	6292 (2)	7307 (1)	2064 (1)	44 (1)
Fe(2)	4813 (2)	7471 (1)	3209 (1)	43 (1)
N(123)	6288 (9)	6687 (7)	3061 (6)	41 (4)
O(123)	7298 (7)	6661 (6)	3698 (5)	49 (3)
N(12)	4990 (9)	8076 (7)	2302 (6)	50 (4)
O(12)	4508 (8)	8824 (6)	2029 (5)	51 (3)
C(1)	4849 (12)	6148 (9)	1228 (9)	52 (5)
O(1)	4345 (9)	6007 (7)	432 (6)	64 (4)
C(2)	3450 (12)	6308 (9)	2252 (7)	45 (5)
O(2)	2281 (7)	6287 (6)	1978 (5)	57 (3)
C(11)	8324 (8)	6999 (6)	1993 (6)	56 (6)
C(12)	7513	6884	1111	62 (6)
C(13)	7046	7870	1061	65 (6)
C(14)	7568	8594	1913	62 (6)
C(15)	8358	8056	2489	58 (5)
C(21)	4328 (9)	8863 (5)	4004 (5)	52 (5)
C(22)	3262	8022	3830	63 (6)
C(23)	3771	7217	4237	58 (6)
C(24)	5151	7560	4663	56 (6)
C(25)	5496	8578	4519	61 (6)
C(31)	3902 (7)	4226 (7)	2365 (6)	63 (6)
C(32)	4114	4082	1490	57 (5)
C(33)	5517	4183	1575	66 (7)
C(34)	6172	4390	2503	59 (6)
C(35)	5174	4417	2991	55 (5)
Me	5453 (16)	4598 (10)	3978 (8)	84 (7)
		B. [K(2,2,2-crypt)]⁺ Monocation		
K	9369 (2)	2140 (2)	2334 (2)	41 (1)
NC(1)	9549 (9)	1757 (7)	4215 (5)	43 (4)
NC(2)	9225 (9)	2506 (7)	474 (5)	43 (4)
OC(1)	11353 (7)	957 (6)	3099 (5)	45 (3)
OC(2)	10923 (7)	1065 (6)	1245 (5)	47 (3)
OC(3)	7090 (7)	1238 (6)	2733 (5)	45 (3)
OC(4)	6874 (7)	1770 (6)	1070 (5)	50 (3)
OC(5)	10098 (7)	3890 (5)	3896 (5)	47 (3)
OC(6)	10232 (7)	4130 (5)	2150 (5)	46 (3)
CC(1)	10739 (11)	1237 (9)	4498 (7)	49 (5)
CC(2)	11002 (11)	449 (9)	3742 (7)	47 (5)
CC(3)	11784 (12)	257 (10)	2418 (7)	57 (5)
CC(4)	12113 (11)	817 (10)	1757 (8)	55 (5)
CC(5)	11176 (11)	1519 (9)	557 (7)	48 (5)
CC(6)	9909 (11)	1707 (9)	−13 (7)	50 (5)
CC(7)	8311 (11)	1080 (9)	4165 (7)	51 (5)
CC(8)	7036 (11)	1355 (10)	3633 (7)	50 (5)
CC(9)	5838 (10)	1379 (10)	2188 (8)	49 (5)
CC(10)	5864 (11)	1088 (9)	1227 (8)	50 (5)
CC(11)	6928 (11)	1526 (10)	155 (8)	56 (5)
CC(12)	7804 (10)	2396 (9)	−14 (7)	44 (4)
CC(13)	9659 (12)	2796 (8)	4850 (7)	47 (5)
CC(14)	10640 (12)	3624 (9)	4725 (7)	50 (5)
CC(15)	10988 (12)	4667 (9)	3739 (7)	51 (5)
CC(16)	10337 (11)	4988 (8)	2900 (7)	40 (4)
CC(17)	9640 (12)	4387 (9)	1322 (7)	48 (5)
CC(18)	9897 (12)	3577 (9)	575 (8)	55 (5)

[a] The equivalent isotropic U is defined as one-third the trace of the orthogonalized $\mathbf{U}_{ij}$ tensor.

trochemical behavior of other triangular metal clusters which contain μ_3-X ligands (where X = CO or NO). Each of the two 48-electron $Co_3(\eta^5\text{-}C_5H_{5-x}Me_x)_3(\mu_3\text{-NO})_2$ clusters (x = 0, 1)[9] exhibits single-electron reversible reduction and oxidation couples. Each of the 49-electron $Ni_3(\eta^5\text{-}C_5H_{5-x}Me_x)_3(\mu_3\text{-CO})_2$ systems (x = 0, 1) also undergoes both a one-electron reduction and a one-electron oxidation.[11b,d] However, 1 differs from the 48-electron (η^5-$C_5H_{5-x}Me_x$)-$CoNi_2(\eta^5\text{-}C_5H_5)_2(\mu_3\text{-CO})_2$ (x = 0, 1) systems which can only undergo reduction to their respective monoanions.[11a]

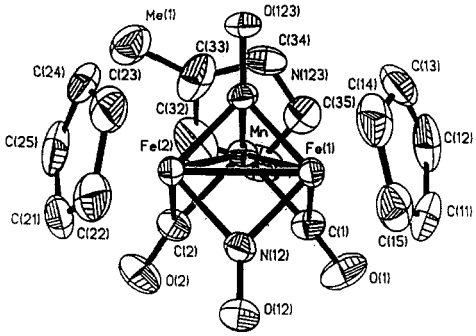

Figure 5. Molecular configuration of (η^5-C_5H_4Me)$MnFe_2$(η^5-C_5H_5)$_2$(μ-CO)$_2$(μ-NO)(μ_3-NO) (1) shown with 50% probability atomic ellipsoids. This 48-electron triangular metal cluster possesses C_1—1 site symmetry.

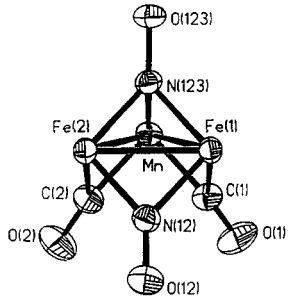

Figure 6. The $MnFe_2$(μ-CO)$_2$(μ-NO)(μ_3-NO) core of 1 which closely conforms to C_s—m symmetry.

Structural Features of (η^5-C_5H_4Me)$MnFe_2$(η^5-C_5H_5)$_2$(μ-CO)$_2$(μ-NO)(μ_3-NO) (1). Views of the entire independent molecule and the $MnFe_2$(μ-CO)$_2$(μ-NO)(μ_3-NO) core of 1 are shown in Figures 5 and 6, respectively. The $MnFe_2$(μ-CO)(μ-NO)(μ_3-NO) core, which closely conforms to C_s—m symmetry, consists of an isosceles triangle of two iron atoms and a manganese atom with each of the two chemically equivalent Mn–Fe edges being bridged by a carbonyl ligand and with the Fe–Fe edge being bridged by a nitrosyl ligand. The $MnFe_2$ triangle is capped by a nitrosyl ligand. The manganese atom was differentiated from the two iron atoms by the coordinating methylcyclopentadienyl ligand; the nitrogen atom of the doubly bridging nitrosyl ligand was unamibiguously differentiated from a carbon atom by a comparison of the resulting refined isotropic thermal parameters when its scattering factor was designated first as a carbon atom and then as a nitrogen atom. A refinement with the scattering factor designated as a carbon atom gave unreasonably low isotropic temperature parameters. Only when the scattering factor of this atom was designated as a nitrogen atom did the thermal motion of this atom become similar to those of the other bridging atoms.

This molecular compound is (to our knowledge) the first example of a mixed-metal cluster containing a triply bridging nitrosyl ligand. The Fe–Fe distance of 2.441 (2) Å and two Mn–Fe distances of 2.555 (2) and 2.567 (2) Å in 1 correspond to single-bond lengths as expected for a 48-electron triangular metal cluster.

A comparison of the molecular geometries of 1 and the electronically equivalent $Mn_3(\eta^5\text{-}C_5H_5)_3(\mu\text{-NO})_3(\mu_3\text{-NO})$ is of interest. Elder[6a] found from his structural determination of $Mn_3(\eta^5\text{-}C_5H_5)_3(\mu\text{-NO})_3(\mu_3\text{-NO})$ that the three independent Mn–(μ_3-NO) bond lengths range from 1.917 (4) to 1.938 (4) Å. The mean of 1.929 Å is significantly longer than the Mn–(μ_3-NO) distance of 1.885 (2) Å found in 1. This difference may be attributed to an electronic effect which reflects the poorer back-bonding ability of the

Table IV. Selected Distances and Bond Angles for $[K(2,2,2\text{-crypt})]^+[(\eta^5\text{-}C_5H_4Me)MnFe_2(\eta^5\text{-}C_5H_5)_2(\mu\text{-}CO)_2(\mu\text{-}NO)(\mu_3\text{-}NO)]^-$

A. Monoanion (1^-)

	Distances (Å)		
Fe(1)–Fe(2)	2.605 (3)	Fe(1)–C(11)	2.197 (9)
Fe(1)–Mn	2.546 (3)	Fe(1)–C(12)	2.186 (10)
Fe(2)–Mn	2.551 (3)	Fe(1)–C(13)	2.145 (11)
Fe(1)–N(123)	1.916 (10)	Fe(1)–C(14)	2.131 (9)
Fe(2)–N(123)	1.937 (10)	Fe(1)–C(15)	2.163 (8)
Mn–N(123)	1.852 (8)		2.164 (av)
Fe(1)–N(12)	1.804 (10)		
Fe(2)–N(12)	1.810 (11)	Fe(2)–C(21)	2.135 (8)
Fe(1)–C(1)	2.025 (10)	Fe(2)–C(22)	2.158 (10)
Mn–C(1)	1.831 (15)	Fe(2)–C(23)	2.205 (10)
Fe(2)–C(2)	2.057 (10)	Fe(2)–C(24)	2.212 (9)
Mn–C(2)	1.853 (13)	Fe(2)–C(25)	2.169 (7)
			2.176 (av)
N(123)–O(123)	1.281 (11)		
N(12)–O(12)	1.245 (13)	Mn–C(31)	2.155 (9)
C(1)–O(1)	1.210 (15)	Mn–C(32)	2.140 (8)
C(2)–O(2)	1.185 (14)	Mn–C(33)	2.168 (9)
		Mn–C(34)	2.199 (9)
C(35)–Mn	1.476 (16)	Mn–C(35)	2.192 (11)
			2.164 (av)
	Bond Angles (deg)		
Fe(1)–Fe(2)–Mn	59.2 (1)	Fe(1)–N(12)–O(12)	134.2 (9)
Fe(2)–Fe(1)–Mn	59.4 (1)	Fe(2)–N(12)–O(12)	133.1 (8)
Fe(1)–Mn–Fe(2)	61.5 (1)	Fe(1)–N(12)–Fe(2)	92.3 (5)
Fe(1)–N(123)–O(123)	127.2 (7)	Fe(1)–C(1)–O(1)	129.8 (10)
Fe(2)–N(123)–O(123)	124.8 (7)	Mn–C(1)–O(1)	147.6 (9)
Mn–N(123)–O(123)	134.1 (7)	Fe(1)–C(1)–Mn	82.5 (5)
Fe(1)–N(123)–Fe(2)	85.1 (4)	Fe(2)–C(2)–O(2)	129.1 (9)
Fe(1)–N(123)–Mn	85.0 (3)	Mn–C(2)–O(2)	149.7 (9)
Fe(2)–N(123)–Mn	84.6 (4)	Fe(2)–C(2)–Mn	81.3 (4)

B. $[K(2,2,2\text{-crypt})]^+$ Monocation

	Distances (Å)		
K–NC(1)	3.077 (10)	NC(1)–CC(7)	1.468 (15)
K–NC(2)	3.040 (10)	CC(7)–CC(8)	1.510 (16)
K–OC(1)	2.873 (8)	CC(8)–OC(3)	1.406 (14)
K–OC(2)	2.844 (8)	OC(3)–CC(9)	1.433 (12)
K–OC(3)	2.804 (8)	CC(9)–CC(10)	1.485 (17)
K–OC(4)	2.811 (7)	CC(10)–OC(4)	1.413 (15)
K–OC(5)	2.872 (7)	OC(4)–CC(11)	1.422 (14)
K–OC(6)	2.762 (8)	CC(11)–CC(12)	1.497 (18)
		CC(12)–NC(2)	1.476 (13)
NC(1)–CC(1)	1.482 (15)		
CC(1)–CC(2)	1.487 (16)	NC(1)–CC(13)	1.476 (13)
CC(2)–OC(1)	1.418 (15)	CC(13)–CC(14)	1.492 (17)
OC(1)–CC(3)	1.430 (14)	CC(14)–OC(5)	1.426 (14)
CC(3)–CC(4)	1.475 (20)	OC(5)–CC(15)	1.409 (15)
CC(4)–OC(2)	1.414 (13)	CC(15)–CC(16)	1.502 (16)
OC(2)–CC(5)	1.403 (15)	CC(16)–OC(6)	1.416 (11)
CC(5)–CC(6)	1.484 (16)	OC(6)–CC(17)	1.431 (14)
CC(6)–NC(2)	1.482 (15)	CC(17)–CC(18)	1.490 (16)
		CC(18)–NC(2)	1.463 (14)
	Bond Angles (deg)		
CC(1)–NC(1)–CC(7)	110.8 (9)	CC(2)–OC(1)–CC(3)	113.0 (9)
CC(1)–NC(1)–CC(13)	109.8 (7)	CC(4)–OC(2)–CC(5)	111.3 (9)
CC(7)–NC(1)–CC(13)	110.3 (9)	CC(8)–OC(3)–CC(9)	110.9 (9)
CC(6)–NC(2)–CC(12)	110.2 (7)	CC(10)–OC(4)–CC(11)	112.3 (8)
CC(6)–NC(2)–CC(18)	109.9 (9)	CC(14)–OC(5)–CC(15)	111.1 (8)
CC(12)–NC(2)–CC(18)	110.3 (9)	CC(16)–OC(6)–CC(17)	111.8 (8)

doubly bridging carbonyl ligands in the $MnFe_2$ cluster as compared to the doubly bridging nitrosyl ligands in the Mn_3 cluster. The resulting larger electron density on the Mn atom in the $MnFe_2$ cluster gives rise to a shorter Mn–(μ_3-NO) distance in **1**.

As was noted by Elder[6a] for $Mn_3(\eta^5\text{-}C_5H_5)_3(\mu\text{-}NO)_3(\mu_3\text{-}NO)$, the lower IR stretching frequency for the triply bridging nitrosyl ligand vs that for the doubly bridging nitrosyl ligands is also reflected in the structure of **1** by a discernible variation in N–O bond length. The N–O bond distance of 1.254 (3) Å for the μ_3-NO ligand is expectedly longer that the 1.212 (3) Å distance associated with the μ-NO ligand.

The two independent Fe–(μ-NO) bond distances of 1.819 (2) and 1.803 (2) Å in **1** are significantly longer than the average Fe–(μ-NO) distance of 1.771 Å found in the $[Fe_2(\eta^5\text{-}C_5H_5)_2(\mu\text{-}NO)_2]^-$ monoanion.[16] The longer Fe–

(16) Kubat-Martin, K. A.; Barr, M. E.; Spencer, B.; Dahl, L. F., *Organometallics*, preceding paper in this issue.

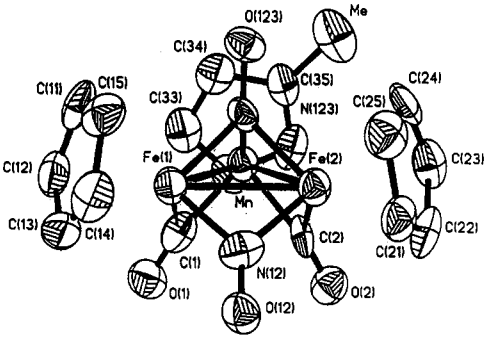

Figure 7. Configuration of the $[(\eta^5\text{-}C_5H_4Me)MnFe_2(\eta^5\text{-}C_5H_5)_2(\mu\text{-}CO)_2(\mu\text{-}NO)(\mu_3\text{-}NO)]^-$ monoanion (1^-) shown with 50% probability atomic ellipsoids. This 49-electron triangular metal cluster possesses C_1—1 site symmetry.

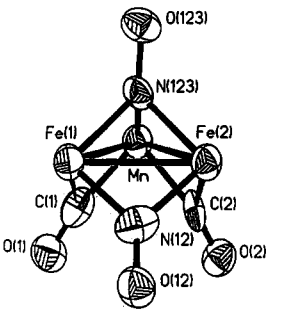

Figure 8. The $MnFe_2(\mu\text{-}CO)_2(\mu\text{-}NO)(\mu_3\text{-}NO)$ core of 1^- which ideally has C_s—m symmetry.

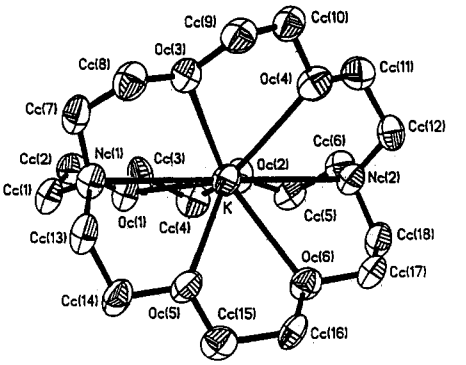

Figure 9. Configuration of the $[K(2,2,2\text{-crypt})]^+$ monocation (where 2,2,2-crypt denotes $N(C_2H_4OC_2H_4OC_2H_4)_3N$) of the 1^- salt shown with 50% probability atomic ellipsoids.

(μ-NO) bond lengths found in **1** can be rationalized on the basis of the competition of the additional π-acceptor carbonyl ligands for electron density, thus weakening the Fe–(μ-NO) bonding interactions.

Structural Features of the $[(\eta^5\text{-}C_5H_4Me)MnFe_2(\eta^5\text{-}C_5H_5)_2(\mu\text{-}CO)_2(\mu\text{-}NO)(\mu_3\text{-}NO)]^-$ Monoanion (1^-): A Comparative Analysis of the Mean Geometries of the 48/49-Electron $[(\eta^5\text{-}C_5H_4Me)MnFe_2(\eta^5\text{-}C_5H_5)_2(\mu\text{-}CO)_2(\mu\text{-}NO)(\mu_3\text{-}NO)]^n$ Series (n = 0, 1–) and Resulting Bonding Implications. A view of the independent 1^- is shown in Figure 7; its $MnFe_2(\mu\text{-}CO)_2(\mu\text{-}NO)(\mu_3\text{-}NO)$ core is shown in Figure 8. The $[K(2,2,2\text{-crypt})]^+$ counterion is displayed in Figure 9. Since the geometry of this counterion has been previously described,[17] it will not be

(17) For example, see: (a) Moras, D.; Metz, B.; Weiss, R. *Acta Crystallogr., Sect. B. Struct. Crystallogr. Cryst. Chem.* **1973**, *B29*, 383–388. (b) Cisar, A.; Corbett, J. D. *Inorg. Chem.* **1977**, *16*, 632–635. (c) Cisar, A.; Corbett, J. D. *Inorg. Chem.* **1977**, *16*, 2482–2487. (d) Belin, C. H. E.; Corbett, J. D.; Cisar, A. *J. Am. Chem. Soc.* **1977**, *99*, 7163–7169. (e) Petersen, J. L.; Brown, R. K.; Williams, J. M. *Inorg. Chem.* **1981**, *20*, 158–165. (f) Chu, C. T.-W.; Lo, F. Y.-K.; Dahl, L. F. *J. Am. Chem. Soc.* **1982**, *104*, 3409–3422.

Table V. Comparison of Selected Mean Distances and Mean Bond Angles for the $[(\eta^5\text{-}C_5H_4Me)MnFe_2(\eta^5\text{-}C_5H_5)_2(\mu\text{-}CO)_2(\mu\text{-}NO)(\mu_3\text{-}NO)]^n$ Series (n = 0 (1), 1- (2)) under Assumed Mirror-Plane Symmetry for the $MnFe_2(\mu\text{-}CO)_2(\mu\text{-}NO)(\mu_3\text{-}NO)$ Fragment

		1 (n = 0)	2 (n = 1-)	diff Δ(2 - 1)
		A. Distances (Å)		
Fe–Fe′	[1][a]	2.441 (2)	2.605 (3)	+0.164
Mn–Fe	[2]	2.561	2.548	−0.013
Fe–(μ-CO)	[2]	2.136	2.041	−0.095
Mn–(μ-CO)	[2]	1.846	1.842	−0.004
Fe–(μ-NO)	[2]	1.811	1.807	−0.004
Fe–(μ_3-NO)	[2]	1.900	1.926	+0.026
Mn–(μ_3-NO)	[1]	1.885 (2)	1.852 (8)	−0.033
Fe–C(ring)	[10]	2.108	2.170	+0.062
Mn–C(ring)	[5]	2.139	2.164	+0.025
		B. Bond Angles (deg)		
Mn–(μ-C)–Fe	[2]	79.6	81.9	+2.3
Fe–(μ-N)–Fe′	[1]	84.7 (1)	92.3 (5)	+7.6
Fe–(μ_3-N)–Fe′	[1]	80.0 (1)	85.1 (4)	+5.1
Mn–(μ_3-N)–Fe	[2]	85.2	84.8	−0.4
Fe–(μ_3-N)–(μ_3-O)	[2]	127.8	126.0	−1.8
Mn–(μ_3-N)–(μ_3-O)	[1]	133.2 (2)	134.1 (7)	+0.9

[a] Brackets enclose the number of equivalent distances whose average values under C_s—m symmetry are listed in the right columns.

discussed here. There are no short contact distances between the monoanion and its counterion indicative of abnormal packing forces or of ion pairing.

The one-electron reduction of **1** to its monoanion (1^-) gives rise to highly significant but yet symmetrical bond-length and bond-angle changes such that the idealized C_s—m architecture of the $MnFe_2(\mu\text{-}CO)_2(\mu\text{-}NO)(\mu_3\text{-}NO)$ core in **1** is maintained in 1^-. The observed geometrical variations under assumed mirror-plane symmetry are presented in Table V. An examination reveals that the Fe–Fe edge of the pseudo-isosceles $MnFe_2$ triangle has considerably enlarged by 0.164 Å from 2.441 (2) Å in **1** to 2.605 (3) Å in 1^-, whereas the two chemically equivalent Mn–Fe edges have slightly decreased by 0.013 Å (av) from 2.561 Å (av) in **1** to 2.548 Å (av) in 1^-. This reduction-induced increase only in the Fe–Fe bond length is consistent with the unpaired electron in 1^- being localized in a MO which is highly antibonding between the two Fe atoms such that this half-filled nondegenerate HOMO (a″ under C_s symmetry) is antisymmetric with respect to the vertical mirror plane.

Under a valence-bond representation, each of the metal–metal interactions in the neutral 48-electron parent (**1**) corresponds to a bond order of 1.0. Localization of the added antibonding electron between the two iron atoms in 1^- with the Mn–Fe bonds being essentially unaltered corresponds to a decrease in metal–metal bond order for the Fe–Fe edge from 1.0 to 0.5.

The distortion of the $MnFe_2$ framework is consistent with each EPR solution spectrum of 1^- exhibiting a single narrow line (29- and 25-G widths at 22 and ~−40 °C, respectively) at g = 1.968 (5). The relative narrowness of the lines and the small deviation of g value from the spin-only value are consistent with the signal arising from a single unpaired electron occupying a nondegenerate MO. Lack of observable hyperfine structure, both in solution and in the glass, suggests little ^{55}Mn (100% abundance, $I = {}^5/_2$) character for this orbital.

The extent of the corresponding changes in the metal–C(ring) distances between **1** and 1^- also reflects localization of the unpaired electron in 1^- mainly on the two iron atoms. The ten Fe–C(ring) distances undergo an average increase from 2.108 Å in **1** to 2.170 Å in 1^-, whereas the five Mn–C(ring) distances undergo an average increase from 2.139 Å in **1** to 2.164 Å in 1^-. This preferential lengthening of the Fe–C(ring) distances by 0.062 Å compared to 0.025 Å for the Mn–C(ring) distances suggests that significant antibonding orbital character exists between the two iron atoms and their coordinated C_5H_5 ligands in the HOMO of 1^-.

Population of the predominantly diiron-antibonding HOMO by the unpaired electron in 1^- also produces a selective effect on the Fe–CO, Fe–NO, and Mn–CO bond lengths of the doubly bridging carbonyl and nitrosyl ligands. Whereas the two longer Fe–CO bonds (2.136 Å (av) in **1** vs 2.041 Å (av) in 1^-) decrease by 0.095 Å upon reduction to 1^-, the two shorter Mn–CO bonds (1.846 Å (av) in **1** and 1.842 Å (av) in 1^-) and the two shorter Fe–NO bonds (1.811 Å (av) in **1** and 1.807 Å (av) in 1^-) remain unchanged (within 0.004 Å).

These bond-length variations may be rationalized from electronic considerations as being an indirect consequence of the negative charge effect which has been previously invoked[11b] to account for the overall energy stabilization of the 49/48-electron $[Ni_3(\eta^5\text{-}C_5H_5)_3(\mu_3\text{-}CO)_2]^n$ series (n = 0, 1+). The addition of the unpaired electron (upon formation of 1^- from **1**) to a HOMO with mainly diiron-based orbital character would lead to a preferential raising of the Fe AO's (relative to a raising of the Mn AO's) nearer in energy to the empty π^*(CO) and π^*(NO) acceptor orbitals and thereby would markedly enhance Fe–CO and Fe–NO back-bonding relative to Mn–CO back-bonding. This increased Fe–CO and Fe–NO back-bonding in 1^- relative to that in **1** is emphasized by a comparison of the solution IR spectra of **1** and 1^-. Upon reduction of **1** to 1^-, there is a considerable decrease in the observed frequencies for the carbonyl and nitrosyl ligands of 83 and 85 cm^{-1} for the two doubly bridging carbonyl groups, 170 cm^{-1} for the doubly bridging nitrosyl group and only 55 cm^{-1} for the triply bridging nitrosyl group.

The observed 0.095-Å average decrease of the two Fe–CO bond lengths and the concurrent nonalteration of the Mn–CO bond lengths upon reduction of **1** to 1^- is in accordance with the above back-bonding arguments involving primarily the iron atoms. However, the fact that the two Fe–NO bond lengths for the doubly bridging nitrosyl ligand are not significantly shorter in 1^- than in **1** is surprising, especially since the above-mentioned IR nitrosyl frequency is 170 cm^{-1} less in 1^-. This virtually unchanged (instead of shorter) mean Fe–NO bond length in 1^- compared to that in **1** may be attributed to the large increase of 0.164 Å in the Fe–Fe distance accompanied by a concomitant large increase of 7.6° in the Fe–N(O)–Fe bond angle for the doubly bridging nitrosyl ligand from 84.7 (1)° in **1** to 92.3 (5)° in 1^-. The resulting obtuse bond angle in 1^- is highly unusual in that the M–N(O)–M bond angles tabulated[18] for a variety of dimers with two doubly bridging nitrosyl ligands range from 81.1° to 86.7°. Both of these extreme distortions in the Fe–Fe distance and the Fe–N(O)–Fe bond angle (upon reduction of **1** to 1^-) would oppose any decrease in the Fe–NO bond lengths especially since such a bond-length decrease would further enlarge the already obtuse Fe–N(O)–Fe bond angle.

Similarly, no change in the mean Fe–NO bond length was previously encountered in the one-electron reduction of the 32-electron $Fe_2(\eta^5\text{-}C_5H_5)_2(\mu\text{-}NO)_2$ to its monoanion[16] (i.e., the mean Fe–NO distance is 1.77 Å in both species). In contrast, a significant shortening of 0.024 Å in the mean

(18) Bottomley, F. *Inorg. Chem.* **1983**, *22*, 2656–2660.

Co–CO bond length was found upon reduction of $Co_2(\eta^5\text{-}C_5Me_5)_2(\mu\text{-}CO)_2$ to its monoanion.[3d] Similar qualitative bonding considerations involving a charge effect were invoked in both of these electronically equivalent iron nitrosyl[16] and cobalt carbonyl[3d] series (n = 0, 1–) in order to account for the increased Fe–NO and Co–CO back-bonding in their monoanions, as indicated by the nitrosyl and carbonyl IR frequencies being decreased by 115 and 80 cm^{-1}, respectively, in their monoanions. In the case of the Fe and Co dimers, it was pointed out that the much stronger Fe–NO bonds should undergo less bond-length decrease than the considerably weaker Co–CO bonds upon increased back-bonding due to reduction. In the case of the 48/49-electron triangular $MnFe_2$ series (n = 0, 1–), one can also speculate that the lack of bond-length change in the Fe–NO bonds for the doubly bridging nitrosyl ligands supports the premise that any change in bond length caused by a charge effect would be much less for the shorter and intrinsically much stronger metal–NO bonds than the corresponding metal–CO bonds.

Upon reduction of 1 to 1^-, all alterations in distances and bond angles involving the triply bridging nitrosyl ligand (Table V) are relatively small, other than the increase in the Fe–(μ_3-N)–Fe′ bond angle of 5.1° which is readily ascribed to the 0.164-Å enlargement in the Fe–Fe′ bond length in 1^-. The capping μ_3-NO ligand is essentially perpendicular to the plane of the $MnFe_2$ triangle in both 1 and 1^-, as evidenced by the angle defined by the N–O vector and the perpendicular vector from the trimetal plane through the nitrogen atom being only 3.1° in 1 and 4.2° in 1^-.

A Comment of the Formation of $[(\eta^5\text{-}C_5H_4Me)MnFe_2(\eta^5\text{-}C_5H_5)_2(\mu\text{-}CO)_2(\mu\text{-}NO)(\mu_3\text{-}NH)]^+$ Monocation (2) from 1. The $MnFe_2(\mu\text{-}CO)_2(\mu\text{-}NO)(\mu_3\text{-}NH)$ core of the 48-electron 2 is geometrically similar to the $MnFe_2(\mu\text{-}CO)_2(\mu\text{-}NO)(\mu_3\text{-}NO)$ core of the 48-electron 1 except for the formal replacement of the oxygen atom in the ON-capped ligand of 1 by the hydrogen atom in the HN-capped ligand of 2.[12] Legzdins and co-workers[19] have isolated the analogous HN-capped $[Mn_3(\eta^5\text{-}C_5H_4Me)_3(\mu\text{-}NO)_3(\mu_3\text{-}NH)]^+$ monocation (which is electronically equivalent with 2) from the reaction of $Mn_3(\eta^2\text{-}C_5H_4Me)_3(\mu\text{-}NO)_3(\mu_3\text{-}NO)$ with excess acid. The $(\mu_3\text{-}NH)^+$-containing product is formed from a protonation of the μ_3-NO ligand in the Mn_3 triangle to first give a cluster possessing a $(\mu_3\text{-}NOH)^+$ ligand. The $(\mu_3\text{-}NOH)^+$-containing intermediate then reacts with another 2 equiv of acid to form the HN-capped triangle (and water). The two electrons which are needed for this process presumably come from a "sacrificial" donation of electrons from the other cluster molecules present in the reaction flask.

In view of these findings,[19] the reaction of the triply bridging nitrosyl ligand in 1 to give the triply bridging imido ligand in 2 by reaction with $AgPF_6$ can be rationalized in terms of an electrophilic attack by Ag^+ on the μ_3-NO ligand. The resulting $(\mu_3\text{-}NOAg)^+$ species could then react with a proton source (adventitious water) and an electron source to form the $(\mu_3\text{-}NH)^+$-containing system. That the Ag^+ ion participates in the interconversion of 1 to 2 is indicated by the fact that reactions of 1 with other oxidizing agents (such as $NOBF_4$) do not yield the HN-capped 2.

Current studies of 2 are underway to determine whether it can also be prepared via protonation of 1 and whether it will display interesting redox chemistry.

Acknowledgment. This research was supported by the National Science Foundation. We are indebted to Dr. R. B. Cody (Nicolet Analytical Instruments) for obtaining a mass spectrum of 1 on a Nicolet FT MS-1000 mass spectrometer. Special thanks are also due to Ms. Mary E. Barr for technical assistance in the chemical part of this research.

Registry No. 1, 110374-77-1; 1^-, 110374-79-3; $1^-[K(2,2,2\text{-crypt})]^+$, 110374-80-6; 1^+, 110374-78-2; 2, 110374-81-7; $Mn(\eta^5\text{-}C_5H_4Me)(CO)_3$, 12108-13-3; $Fe_2(\eta^5\text{-}C_5H_5)(\mu\text{-}NO)_2$, 52124-51-3; Mn, 7439-96-5; Fe, 7439-89-6.

Supplementary Material Available: Figure 1, an infrared spectrum (KBr disk) of $(\eta^5\text{-}C_5H_4Me)MnFe_2(\eta^5\text{-}C_5H_5)_2(\mu\text{-}CO)_2(\mu\text{-}NO)(\mu_3\text{-}NO)$ (1), Figure 3, the IR spectral changes in the carbonyl region upon reduction of 1 in THF to its monoanion (1^-), and tables with coordinates and isotropic temperature factors for the hydrogen atoms and anisotropic thermal parameters for the non-hydrogen atoms (8 pages); a listing of observed and calculated structure factor amplitudes for both compounds (39 pages). Ordering information is given on any current masthead page.

(19) Lgezdins, P.; Nurse, C. R.; Rettig, S. J. *J. Am. Chem. Soc*, **1983**, *105*, 3727–3728.